Robust Optimal Operation Method for Active Distribution Networks with Multiple Types of Regulation Resources Considering Source and Load Uncertainties

Ran DING [1,2], Lin CHENG [1,3,4], Xuanyuan WANG [2], Yiming YAO [2], Haixiang XU [2], Ergang ZHAO [4]*

[1] Dept. of Electrical Engineering, Tsinghua University, Haidian District, Beijing, China
[2] State Grid Jibei Electric Power Company Limited, Xicheng District, Beijing, China
[3] State Key Laboratory of Power System Operation and Control, Dept. of Electrical Engineering, Tsinghua University, Haidian District, Beijing, China
[4] Wuxi Institute of Applied Technology, Tsinghua University, Wuxi City, Jiangsu Province, China

64353346@qq.com, chenglin@mail.tsinghua.edu.cn, wang.xuanyuan@jibei.sgcc.com.cn, yaoym01@163.com, xhx0617@foxmail.com, zhaoeg10@163.com*

Submitted November 13, 2024 / Accepted February 10, 2025 / Online first March 10, 2025

Abstract. *The increasing prevalence of renewable energy sources and the heightened uncertainty in load demands within active distribution networks (ADNs) have led to more fluctuations in power flow and voltage levels during operational periods. In light of these challenges, this paper proposes a robust optimization framework specifically designed for ADNs, which carefully balances system security, economic efficiency, and operational flexibility with multiple types of regulation resources. Firstly, a comprehensive regulation methodology is employed to integrate a variety of dispatchable resources. Secondly, the proposed model accounts for the inherent uncertainties related to load demand and the output of renewable energy generation by using the robust optimization (RO) technique. The proposed robust operational model for ADNs aims to minimizing power losses within the network and reducing voltage deviations, thereby improving overall network performance and reliability. Thirdly, the proposed model is linearized and reformulated as a convex optimization problem utilizing second-order cone relaxation techniques, and a relaxed cooperative co-evolution algorithm is implemented to solve it efficiently. Numerical results across various scenarios indicate that, compared to the conventional model without regulation resources, the proposed robust optimization model with multiple types of regulation resources can reduce voltage fluctuations by 89.6% and network losses by 12.9%. The proposed algorithm demonstrates better computational performance compared to conventional methods.*

Keywords

Active distribution networks, renewable energy integration, dispatch resources, source and load uncertainties, second-order cone relaxation techniques

1. Introduction

Recent developments in renewable energy sources (RESs) and an increase in the unpredictability of power loads have introduced considerable volatility, which has resulted in reverse power flows, voltage fluctuations, and frequent violations of operational limits within distribution networks [1],[2]. The uncertainties arising from both generation and consumption sides can lead to the operation of distribution networks under complex and extreme conditions, complicating the tasks of reactive power and voltage regulation, and potentially jeopardizing the safety and stability of the network [3]–[5]. The significant integration of RESs, electric vehicles (EVs), and energy storage systems (ESSs) into power infrastructures necessitates the extensive implementation of various flexible electronic devices. These devices enable the dynamic and efficient management of these emerging components, providing enhanced functionalities for power management and voltage stabilization. Consequently, they play a crucial role in increasing system flexibility and strengthening grid resilience against fluctuations and disturbances [6]–[8]. Recently, the application of flexible power electronic technologies in distribution networks has been on the rise [9]. These technologies present effective solutions to mitigate the high volatility associated with renewable energy generation and the randomness of load demands, thereby alleviating issues related to transmission congestion within distribution networks.

The effective management of distribution networks, particularly in the context of integrating RESs and regulating voltage, relies on various regulatory resources, including capacitor banks (CBs), static var compensators (SVCs), network reconfiguration, and ESSs [10]–[13]. CBs contribute to voltage stability by providing reactive power compensation, while SVCs offer rapid responses to voltage

DOI: 10.13164/re.2025.0037

fluctuations, thereby enhancing the dynamic equilibrium of the grid. Network reconfiguration serves to optimize the distribution of power flow, thereby increasing system flexibility. Additionally, ESSs exhibit significant efficiency in peak shaving, mitigating fluctuations in renewable energy output, and maintaining grid stability. In [10], a model predictive control (MPC)-based methodology is introduced for voltage regulation that optimally adjusts the reactive power outputs of generators and SVCs to uphold power system stability. This approach employs a sensitivity-informed state-space model and seeks to minimize a cost function while adhering to Voltage Stability Indices (VSIs) and operational constraints. An advanced energy management dispatch (EMD) strategy designed for the coordination of ESSs powered by batteries and renewable energy sources within medium-voltage distribution networks is presented in [11]. This methodology utilizes a convex approximation to enhance the dispatch optimization process, thereby ensuring operational efficiency and economic viability. The enhancement of distribution system efficiency through hybrid reconfiguration and coordinated operation of distributed generation (DG) has been discussed in [12], which can reduce power losses; however, the significant effects of voltage fluctuations on load power and DG output are frequently neglected, necessitating the use of complex nonlinear or linearization techniques. Reference [13] aims to investigate the coordinated impact of flexible technologies, including renewable-based distributed generations, battery energy storage systems, controllable load management, and network reconfiguration, on enhancing distribution system performance despite various technical constraints. In summary, these resources contribute to the effective integration of RESs and voltage regulation within distribution networks, facilitating more intelligent and reliable operations of power systems.

The Soft Open Point (SOP) represents an advanced power electronic device that facilitates continuous reactive power compensation, thereby improving power balance and voltage regulation within ADNs [14], [15]. In comparison to conventional switching devices, the SOP demonstrates superior response times, extended operational lifespans, and enhanced capacity for managing impulse currents, rendering it particularly suitable for the integration of intermittent renewable energy sources [16]. In [14], an SOP operational strategy that has been optimized through particle swarm optimization to enhance voltage stability in ADNs is presented, while taking into account both network and technical constraints. The deep reinforcement learning method is employed in [15] to facilitate efficient real-time decision-making in the reconfiguration of ADNs that incorporate SOPs and large-scale distributed generation. A robust mixed-integer convex optimization model is introduced in [17], aimed at optimal SOP scheduling in conjunction with energy storage systems, focusing on the management of power flows, minimization of losses, and maximization of profits within ADNs, while addressing uncertainties associated with demand and renewable generation. A three-stage optimization approach is proposed in [18] to synchronize SOPs with other active management strategies in ADNs, specifically targeting voltage fluctuations induced by variations in photovoltaic power through scheduled adjustments, periodic optimization, and real-time control. Although these studies have advanced the application of SOPs in ADNs, there remains a lack of research addressing the collaborative optimization of SOPs alongside other regulatory resources such as CBs, SVCs, and network reconfiguration.

The uncertainties arising from both energy supply and demand contribute to increasingly complex and unpredictable power flow dynamics within ADNs. Traditional deterministic optimization models may fall short in adequately addressing the safety and economic requirements across a range of operational scenarios influenced by these uncertainties. Consequently, robust optimization (RO) and stochastic programming (SP) have emerged as effective methodologies for addressing challenges associated with uncertainty. In [19], a two-phase optimization strategy is introduced based on particle swarm optimization for ADNs, with the objective of reducing operational costs and minimizing load shedding while accounting for uncertainties in renewable energy sources, demand, pricing, and system reliability. In [20], a stochastic programming approach for the coordination of distributed energy resources (DERs) in unbalanced ADNs is proposed to address operational uncertainties. A robust multi-objective optimization framework for ADNs is delineated in [21], emphasizing the enhancement of renewable energy utilization and the reduction of losses through the effective management of photovoltaic output uncertainties via scenario analysis and the generation of Pareto fronts. A trilevel, two-stage robust optimization model, referred to as Defender-Attacker-Defender (DAD), is developed in [22], which aims to optimally pre-allocate and dispatch defensive resources in the face of three types of uncertainties—attack strategies, wind power, and solar irradiation—thereby minimizing load shedding. This model leverages energy storage capacity and is solved using a Column and Constraint Generation (C&CG) algorithm with Second Order Cone Programming (SOCP) relaxation for non-convex sub-problems. Current research predominantly addresses robust optimization challenges through the C&CG method or by reformulating them into general optimization problems via duality. Nevertheless, there is a need for enhancements in the complexity, computational efficiency, and worst-case scenario identification of the C&CG algorithm.

In response to existing challenges, this study presents a comprehensive operational model for ADNs, prioritizing system security, economic efficiency, and operational flexibility. A comparison of the proposed model with the related studies is provided in Tab. 1. The proposed model is designed to thoroughly incorporate uncertainties associated with load variations and renewable energy generation. The main contributions of this paper can be summarized as follows:

Ref.	DG	Reactive power compensation device	ESSs	SOP	Reconfiguration	Robust optimization
[10]	✓	✓	×	×	×	×
[11]	✓	×	✓	×	×	×
[12]	✓	×	×	×	✓	×
[13]	✓	✓	✓	×	✓	×
[14]	✓	×	×	✓	×	×
[15]	✓	×	×	✓	✓	×
[17]	✓	×	✓	✓	×	✓
[21]	✓	×	×	×	×	✓
This study	✓	✓	✓	✓	✓	✓

Tab. 1. Related studies and key features of this study.

- Compared with existing studies, this paper integrates a wide range of regulatory resources, such as distributed generation, energy storage systems, reactive power compensation devices, and flexible network reconfiguration strategies. This integration serves as the foundation for a robust optimal operational framework for ADNs, with the primary goals of minimizing network losses and reducing voltage fluctuations. The proposed model effectively balances operational cost and voltage regulation, thereby ensuring optimal performance of the network.
- The proposed model undergoes linearization through second-order cone relaxation techniques, transforming it into a convex optimization problem. This transformation not only simplifies the model but also enhances the efficiency of its solution process. To address the resulting optimization problem, a relaxation evolutionary algorithm is utilized, providing a robust approach for tackling complex optimization challenges.
- A comparative analysis is conducted against a traditional robust optimization algorithm to highlight the improved efficacy and precision of the proposed algorithm. The impacts of uncertainties in renewable energy supply and demand on the system are also investigated under different scenario settings.

The subsequent sections of this paper are structured as follows: Section 2 provides an overview of the modeling of various regulatory resources. Section 3 introduces the proposed robust optimal operation model for ADNs. The linearization of the model and the corresponding solution methodology are detailed in Sec. 4. Section 5 presents and discusses the results of the case study. Finally, this paper is concluded in Sec. 6.

2. Modeling of Multiple Regulation Resources

In order to mitigate the volatility and uncertainty associated with renewable energy sources and load demands, distribution networks implement a range of regulatory resources as active management strategies. These resources include Soft Open Points (SOPS) equipped with an energy storage system (ESS), SVCs, CBs, and network reconfiguration techniques.

2.1 Modeling of SOPS

A SOP enhances the flexibility and power quality of distribution networks by functioning as a controllable switch that regulates bidirectional power flow. It facilitates the rerouting of power, balances load distributions, and addresses challenges such as congestion and voltage sags through precise control of phase angles and voltage magnitudes. The SOP typically exists in two primary configurations: the two-terminal SOP and the three-terminal SOP. These configurations enable the simultaneous connection of either two or multiple feeders, respectively, thereby improving the connectivity and adaptability of distribution networks.

The integration of a SOPS significantly optimizes grid performance. The SOP effectively manages power flow, which is essential for maintaining microgrid stability and addressing peak demand periods, while the ESS contribute to load curve smoothing and reduces reliance on costly peaking power plants. Both components play a vital role in voltage regulation, with the SOP adjusting phase angles and the ESS managing reactive power. In scenarios involving isolated grids, this system facilitates island operation and supports critical load requirements. Furthermore, it enhances the integration of renewable energy by balancing intermittent supply, storing surplus energy, and directing power to areas of high demand. During fault conditions, the ESS provides immediate power availability, while the SOP efficiently redirects power. By participating in ancillary services, the system optimizes operational efficiency, generates revenue, and supports dynamic demand response mechanisms to avert blackouts.

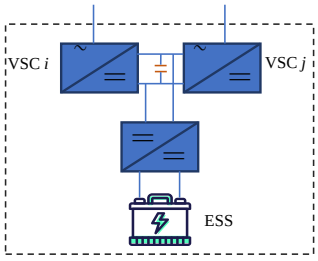

Fig. 1. Illustration of a two-terminal SOP with an ESS.

Consequently, a system design that combines a two-terminal SOP with an ESS is employed, as illustrated in Fig. 1. This configuration utilizes two voltage source converters (VSCs) connected by a DC-DC converter, with an attached battery for energy storage and retrieval, thereby optimizing usage and enhancing flexibility. This arrangement facilitates controlled power exchange between feeders and efficient energy storage management.

Mathematically, the SOP and ESS are modeled with constraints that reflect their operational limits and characteristics, including power flow constraints, reactive power capabilities, energy storage capacity, power ratings, and depth of discharge, ensuring that the system operates efficiently and reliably across various operational conditions. Constraint (1) updates the state of energy storage $S_{i,t}$, taking into account the energy generated during the charging process and the energy utilized during discharging. Constraint (2) stipulates that the initial state of charge (SOC) at the beginning of the period must be equivalent to the final state at the conclusion of the period. Furthermore, constraints (3)-(4) dictate that the charging and discharging power of battery i at time t must fall within the range of 0 to its maximum charging and discharging capacity ($p_i^{\text{cha,max}}/p_i^{\text{dis,max}}$). Constraint (5) guarantees that the total power flow from the ESS, aggregated across all batteries i within the set Ω^{P} at time t, is equal to the net difference between discharging and charging power. Constraint (6) ensures that the apparent power of the SOPS at time t does not surpass its rated capacity (S^{SOP}). Additionally, the reactive power $Q_{i,t}^{\text{SOP}}$ is bounded by its physical minimum and maximum limits.

$$S_{i,t+1} = S_{i,t} + p_{i,t}^{\text{cha}}\eta^{\text{cha}} - p_{i,t}^{\text{dis}}/\eta^{\text{dis}}, \tag{1}$$

$$S_{i,1} = S_{i,T}, \tag{2}$$

$$0 \le p_{i,t}^{\text{cha}} \le b_{i,t}^{\text{cha}} p_i^{\text{cha,max}}, \tag{3}$$

$$0 \le p_{i,t}^{\text{dis}} \le \left(1 - b_{i,t}^{\text{cha}}\right) p_i^{\text{dis,max}}, \tag{4}$$

$$\sum_{i\in\Omega^{\text{P}}} P_{i,t}^{\text{SOP}} = p_{i,t}^{\text{dis}} - p_{i,t}^{\text{cha}}, \tag{5}$$

$$\sqrt{\left(P_{i,t}^{\text{SOP}}\right)^2 + \left(Q_{i,t}^{\text{SOP}}\right)^2} \le S^{\text{SOP}} \tag{6}$$

where $p_{i,t}^{\text{cha}}$ and $p_{i,t}^{\text{dis}}$ denote the charging/discharging power of ESS at time t, respectively. η^{cha} and η^{dis} are the charging/discharging efficiencies. Additionally, $S_{i,t}$ remains within specified minimum and maximum limits. The binary variable $b_{i,t}^{\text{cha}}$ denotes whether the battery is in a charging state (1) or not (0).

2.2 Modeling of SVC

An SVC represents a sophisticated element within contemporary power systems, specifically engineered to deliver dynamic reactive power support, as illustrated in Fig. 2. In contrast to conventional devices, the SVC provides continuous reactive power compensation ($Q_{i,t}^{\text{SVC}}$), thereby effectively regulating voltage and sustaining grid stability. Similarly, the SVC needs to satisfy its upper and lower bounds during operation.

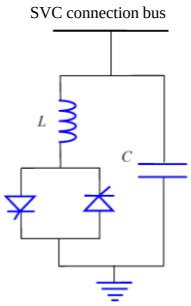

Fig. 2. Illustration of the SVC structure.

2.3 Modeling of CB

Conversely, CBs are categorized as discrete reactive power compensation devices that function as slower-speed regulation resources. Although they are proficient in compensating for reactive power and stabilizing voltage levels within power systems, their operation is characterized by a stepped approach, necessitating a longer adjustment period compared to the continuously variable nature of SVCs. The reactive power output of the capacitor $Q_{i,t}^{\text{CB}}$ is articulated in (7). Constraint (8) limits the total number of switching operations σ^{CBmax} (steps up or down) that capacitor bank i can execute throughout the entire time horizon T. Indeed, the number of steps of capacitor bank i connected to the system at time t remains within its physical limit.

$$Q_{i,t}^{\text{CB}} = Z_{i,t}^{\text{CB}} Q^{\text{CB,step}}, \tag{7}$$

$$\sum_{t=1}^{T-1} \left| Z_{i,t+1}^{\text{CB}} - Z_{i,t}^{\text{CB}} \right| \le \sigma^{\text{CBmax}} \tag{8}$$

where the variable $Z_{i,t}^{\text{CB}}$ denotes a discrete control variable that indicates the number of steps (or units) of capacitor bank i that are engaged with the system at time t. $Q^{\text{CB,step}}$ means the capacity of one step or unit.

2.4 Modeling of Network Reconfiguration

In the context of a distribution network, network reconfiguration serves as a vital strategy employed by network operators to enhance system performance. This process entails modifying the network topology by managing the state of contact switches—such as breakers, reclosers, and sectionalizers—that interconnect various segments of the network. By judiciously opening or closing these switches, operators can modify the direction and distribution of power flow to achieve multiple objectives, including loss minimization, reliability maximization, voltage profile enhancement, or isolation of malfunctioning sections. Network reconfiguration is governed by a series of constraints to ensure the system's operational integrity and safety. Specifically, constraint (9) applies Kirchhoff's Cur-

rent Law to each node j, excluding the reference node (node 1). The negative sign indicates that any power injection at the node results in a reduction of the net flow into that node. Constraint (10) establishes the equivalence between the cumulative power output from the reference node (node 1) directed towards its connected child nodes k and the total power demand or generation λ_v at that particular node. Constraint (11) delineates the limitations on power flow $F_{ij,t}$ through line ij at time t. Constraint (12) ensures that precisely $n-1$ lines are closed at any time t (where n represents the number of nodes in the network), and constraint (13) restricts the frequency with which a specific line ij can transition between open and closed states throughout the optimization horizon $T-1$. Furthermore, constraint (14) imposes a cap on the total number of switching operations permissible across the entire network during the optimization horizon $T-1$.

$$\sum_{k\in c(j)} F_{jk,t} - \sum_{i\in d(j)} F_{ij,t} = -F_{j,t},\ j \neq 1, \tag{9}$$

$$\sum_{k\in c(1)} F_{1k,t} = \lambda_v, \tag{10}$$

$$-MZ^{\mathrm{L}}_{ij,t} \le F_{ij,t} \le MZ^{\mathrm{L}}_{ij,t}, ij \in \Omega^{\mathrm{L}}, \tag{11}$$

$$\sum_{ij\in\Omega^{\mathrm{L}}} Z^{\mathrm{L}}_{ij,t} = n-1, \tag{12}$$

$$\sum_{t=1}^{T-1} \left| Z^{\mathrm{L}}_{ij,t+1} - Z^{\mathrm{L}}_{ij,t} \right| \le Z^{\mathrm{Lmax}}, \tag{13}$$

$$\sum_{t=1}^{T-1} \sum_{j\in\Omega^{\mathrm{L}}} \left| Z^{\mathrm{L}}_{ij,t+1} - Z^{\mathrm{L}}_{ij,t} \right| \le Z^{\mathrm{sLmax}} \tag{14}$$

where M is a large positive constant. $Z^{\mathrm{L}}_{ij,t}$ represents the status of the line connecting nodes i and j at time t, where 1 indicates the line is closed and 0 indicates it is open. Ω^{L} is the set of all lines. $\left| Z^{\mathrm{L}}_{ij,t+1} - Z^{\mathrm{L}}_{ij,t} \right|$ represents the change in the status of the line connecting nodes i and j between consecutive time steps. Z^{Lmax} and Z^{sLmax} represent the limits of one single and all contact switches.

3. Robust Optimal Operation Model for ADNs

In the context of managing a distribution network, uncertainties such as fluctuations in load and the variability of renewable energy generation present considerable challenges that can adversely affect service quality and operational efficiency. These uncertainties introduce variability within the network, which may result in significant voltage deviations and increased network losses. Voltage deviation, defined as the difference between the actual voltage at any point in the network and the nominal voltage level, is a critical parameter that necessitates careful monitoring and control. Excessive voltage deviations can degrade power quality, thereby affecting the performance of connected electrical devices and diminishing customer satisfaction. Conversely, total network loss, primarily resulting from the resistive characteristics of conductors that lead to energy dissipation as heat, contributes to inefficiencies, elevated operational costs, and a heightened environmental impact.

To address these challenges, RO techniques, which are specifically tailored to manage uncertain parameters, are employed. In this context, a min-max optimization framework is particularly advantageous, as it seeks to minimize the worst-case scenarios for both voltage deviation and network loss, thereby ensuring stable power quality and operational efficiency across a spectrum of uncertain conditions. This methodology enables network operators to make decisions that are resilient to the variability introduced by load fluctuations and renewable energy output, thereby enhancing the overall reliability and sustainability of the distribution network.

3.1 Objective Function

The formulation of the robust optimal operation model specific to ADNs involves the establishment of equations and the delineation of the objective function, i.e., equations (15) and (16). This constitutes a minimax problem, wherein the primary aim is to minimize the maximum potential value of the function f, taking into account two distinct sets of variables: x from $\boldsymbol{X}$, representing the domain of decision variables, and y from $\boldsymbol{Y}$, denoting the domain of uncertain variables. This dual-variable optimization approach seeks to achieve a balance that yields the most robust solution, accommodating both controllable decisions and potential uncertainties. The problem is designed to identify the optimal strategy under worst-case scenarios, which is essential in uncertain environments where it is necessary to mitigate against potential adverse situations or extreme conditions. In this framework, f is defined as the overall objective function, represented as a weighted sum of two sub-objectives, f_1 and f_2. The weights α and β are utilized to balance the significance of each sub-objective, with μ serving as a scaling factor (commonly referred to as a dimensional uniform conversion scaling coefficient) to ensure uniformity in the conversion of measurements across different dimensions.

$$\min_{x\in\mathbf{X}} \max_{y\in\mathbf{Y}} f \tag{15}$$

$$\begin{cases} f = \alpha f_1 + \beta\mu f_2 \\ f_1 = \sum_{t=1}^{T-1} \sum_{i\in d(j)} r_{ij} I^2_{ij,t} \Delta t \\ f_2 = \sum_{t\in T} \sum_{i\in n} \left| \dfrac{U^2_{i,t} - U^2_{\mathrm{N}}}{U^2_{\mathrm{N}}} \right| \\ \alpha + \beta = 1 \end{cases} \tag{16}$$

where r_{ij} represents the resistance of line ij, $I_{ij,t}$ denotes the current flowing through line ij at time t, $U_{i,t}$ indicates the voltage at bus i at time t, and U_{N} signifies the rated voltage of the system. The constraint $\alpha + \beta = 1$ guarantees that the total weight is normalized, reflecting a coherent combina-

tion of objectives. Specifically, f_1 pertains to the minimization of total network losses, while f_2 focuses on minimizing the deviation of nodal voltages from their nominal values. The optimization problem thus aims to identify the optimal operational strategy that minimizes total network losses while concurrently maintaining voltage deviations at minimal levels, all under the assumption of worst-case scenarios for certain parameters, likely represented by the variables *y*. The trade-off between these two objectives is modulated by the parameters α and β, allowing for adaptable prioritization based on the specific operational requirements or constraints of the power system.

Furthermore, constraints (17)–(21) are employed to articulate the uncertainties associated with both sources and loads. In particular, the set of uncertain variables $\boldsymbol{Y}$ can be characterized by the predicted value $y_{j,t}^{\text{pre}}$, the maximum value $y_{j,t}^{\max}$, and the minimum value $y_{j,t}^{\min}$. Constraints (18) and (19) delineate the methodology for calculating the maximum and minimum adjusted values of *y* at node *j* and time *t*. Specifically, they scale the prior value $y_{j,t}^{\text{pre}}$ by factors of $(1 + \omega)$ and $(1 - \omega)$. A particular constraint ensures that at most one of $\lambda_{j,t}^{+}$ or $\lambda_{j,t}^{-}$ can be non-zero for any given *j* and *t*, thereby preventing the simultaneous increase and decrease of the variable *y*. Another constraint imposes a limit on the total number of adjustments (either increases or decreases) that *y* can undergo throughout the entire time horizon *T* for a specified node *j*.

$$\boldsymbol{Y} = \left(1-\lambda_{j,t}^{+}-\lambda_{j,t}^{-}\right) y_{j,t}^{\text{pre}} + \lambda_{j,t}^{+} y_{j,t}^{\max} + \lambda_{j,t}^{-} y_{j,t}^{\min}, \tag{17}$$

$$y_{j,t}^{\max} = \left(1+\omega\right) y_{j,t}^{\text{pre}}, \tag{18}$$

$$y_{j,t}^{\min} = \left(1-\omega\right) y_{j,t}^{\text{pre}}, \tag{19}$$

$$\lambda_{j,t}^{+} + \lambda_{j,t}^{-} \le 1, \tag{20}$$

$$\sum_{t\in T}\left(\lambda_{j,t}^{+} + \lambda_{j,t}^{-}\right) \le \Lambda_j \tag{21}$$

where the binary variables $\lambda^{+}_{j,t}$ or $\lambda^{-}_{j,t}$ denote decisions regarding the potential increase or decrease of the variable *y* at node *j* and time *t*. ω signifies the permissible percentage change expressed as a decimal value. ω is used to adjust the range of the interval, and a larger omega indicates a larger uncertainty interval. The parameter Λ_j indicates the maximum number of adjustments permitted for *y* at node *j*.

3.2 Constraints

Constraints (1)-(14) establish the operational limits of the regulatory resources implemented. Additional constraints are outlined as follows:

1. Power Flow Constraints Considering Network Reconfiguration

The traditional DistFlow model requires modification when accounting for network reconfiguration. Constraint (22) articulates the conservation of active and reactive power at node *j* at time *t*, asserting that the power output, minus losses, equals the power input plus the power injected at the node. Inequalities in (23) link the squared voltages at nodes *i* and *j* to the active and reactive powers traversing the line connecting them, utilizing the big-M method with the binary variable $Z^{\text{L}}_{ij,t}$ to indicate whether the line is closed or open. The final equation computes the magnitude of the current. Constraint (24) is defined to establish the power balance at node *j* at time *t*.

$$\begin{cases} \sum_{i\in d(j)}\left(P_{ij,t} - I_{ij,t}^2 r_{ij}\right) - P_{j,t} = \sum_{k\in c(j)} P_{jk,t} \\ \sum_{i\in d(j)}\left(Q_{ij,t} - I_{ij,t}^2 x_{ij}\right) - Q_{j,t} = \sum_{k\in c(j)} Q_{jk,t} \end{cases} \tag{22}$$

$$\begin{cases} U_{i,t}^2 - U_{j,t}^2 \ge 2\left(r_{ij}P_{ij,t} + x_{ij}Q_{ij,t}\right) - M\left(1-Z_{ij,t}^{\text{L}}\right) - I_{ij,t}^2\left(x_{ij}^2 + r_{ij}^2\right) \\ U_{i,t}^2 - U_{j,t}^2 \le 2\left(r_{ij}P_{ij,t} + x_{ij}Q_{ij,t}\right) + M\left(1-Z_{ij,t}^{\text{L}}\right) - I_{ij,t}^2\left(x_{ij}^2 + r_{ij}^2\right) \\ I_{ij,t}^2 = \dfrac{\left(P_{ij,t}^2 + Q_{ij,t}^2\right)}{U_{i,t}^2} \end{cases} \tag{23}$$

$$\begin{cases} P_{j,t} = P_{j,t}^{\text{Load}} - P_{j,t}^{\text{DG}} - P_{j,t}^{\text{Grid}} - P_{j,t}^{\text{SOP}} \\ Q_{j,t} = Q_{j,t}^{\text{Load}} - Q_{j,t}^{\text{DG}} - Q_{j,t}^{\text{Grid}} - Q_{j,t}^{\text{SOP}} - Q_{j,t}^{\text{SVC}} - Q_{j,t}^{\text{CB}} \end{cases} \tag{24}$$

where $P_{ij,t}$ and $Q_{ij,t}$ are the active and reactive power transmitted by line *ij* at time *t*, respectively. x_{ij} is the reactance of line *ij*. $P_{j,t}$ and $Q_{j,t}$ are the net injected active and reactive power at bus *j* at time *t*. Similarly, $P_{jk,t}$ and $Q_{jk,t}$ are the active and reactive power transmitted by line *jk* at time *t*. $P_{j,t}^{\text{DG}}$ and $Q_{j,t}^{\text{DG}}$ represent the active and reactive power generated by renewable energy sources at bus *j* at time *t*. $P_{j,t}^{\text{Grid}}$ and $Q_{j,t}^{\text{Grid}}$ represent the active and reactive power supplied by the substation at bus *j* at time *t*. $P_{i.t}^{\text{Load}}$ and $Q_{i.t}^{\text{Load}}$ represent the active and reactive power consumed by the load at bus *j* at time *t*.

2. Substation Operational Constraints

Given the finite capacity of ADNs, the transmission of power from the main grid to these networks via substations necessitates meticulous management. In particular, while supplying active power, substations must also regulate the exchange of reactive power to ensure that the total power throughput remains within designated limits. This regulation is crucial for mitigating the effects of power fluctuations within DNs on the stability of the main grid. The pair of inequalities in (25) delineate the acceptable ranges for the active and reactive power outputs of substation *i* at any given time *t*, thereby protecting against potential overloads and ensuring operational integrity.

$$\begin{cases} P^{\text{Grid,min}} \le P_{i,t}^{\text{Grid}} \le P^{\text{Grid,max}} \\ Q^{\text{Grid,min}} \le Q_{i,t}^{\text{Grid}} \le Q^{\text{Grid,max}} \end{cases} \tag{25}$$

where $P^{\text{Grid,max}}$ / $P^{\text{Grid,min}}$ and $Q^{\text{Grid,max}}$ / $Q^{\text{Grid,min}}$ are the upper/lower bounds on the active and reactive power outputs.

3. DG Operational Constraints

Constraint (26) defines the permissible limits for both active and reactive power outputs for DG unit *i* at a given time *t*.

$$\begin{cases} P_{i,t}^{\mathrm{DGmin}} \le P_{i,t}^{\mathrm{DG}} \le P_{i,t}^{\mathrm{DGmax}} \\ Q_{i,t}^{\mathrm{DG}} = P_{i,t}^{\mathrm{DG}} \times \tan\theta \\ \tan\theta = \dfrac{\sqrt{1-\cos\theta^2}}{\cos\theta} \end{cases} \tag{26}$$

where $P_{i,t}^{\mathrm{DGmax}}$ and $P_{i,t}^{\mathrm{DGmin}}$ are the upper/lower bounds of the DG active power output. $\cos\theta$ is the power factor.

4. System Security Constraints

In the context of ADN operations, it is imperative to maintain bus voltages within specified limits to ensure the proper functioning of equipment and the quality of power supplied. Additionally, managing branch currents and transmission powers is essential to prevent overloading, equipment malfunctions, and service interruptions, thereby preserving the reliability and efficiency of the network. This necessitates ongoing monitoring and control to ensure that all operational variables (e.g., the voltage magnitude $U_{i,t}$, the current $I_{ij,t}$, active and reactive power flow $P_{ij,t}$ / $Q_{ij,t}$) remain within safe limits, thereby optimizing network performance.

4. Model Linearization and Solution Method

As highlighted in the preceding discussion, the model formulated encompasses various nonlinear and nonconvex elements, which complicates its direct resolution using traditional optimization solvers. To address this issue, the current section initiates the process by linearizing the nonlinear components, thereby enabling their approximation through linear equivalents, which enhances the model's tractability. Subsequently, second-order cone relaxation techniques are employed to reformulate the model into a MISOCP format, facilitating its resolution with specialized optimization algorithms.

4.1 Model Linearization

To address the squared terms of voltage and current present in the constraints, we introduce new variables, $l_{ij,t}$ and $V_{i,t}$, to substitute these terms, as shown in (27).

$$\begin{cases} I_{ij,t}^2 = l_{ij,t} \\ U_{i,t}^2 = V_{i,t} \end{cases} \tag{27}$$

Then, constraints (16), (22), and (23) can be replaced by the following forms.

$$\begin{cases} f = \alpha f_1 + \beta\mu f_2 \\ f_1 = \sum_{t=1}^{T-1} \sum_{i\in d(j)} r_{ij} l_{ij,t} \Delta t \\ f_2 = \sum_{t\in T} \sum_{i\in n} \left| \dfrac{V_{i,t} - V_{\mathrm{N}}}{V_{\mathrm{N}}} \right| \\ \alpha + \beta = 1 \end{cases} \tag{28}$$

$$\begin{cases} \sum_{i\in d(j)} \left(P_{ij,t} - l_{ij,t} r_{ij} \right) - P_{j,t} = \sum_{k\in c(j)} P_{jk,t} \\ \sum_{i\in d(j)} \left(Q_{ij,t} - l_{ij,t} x_{ij} \right) - Q_{j,t} = \sum_{k\in c(j)} Q_{jk,t} \end{cases} \tag{29}$$

$$\begin{cases} V_{i,t} - V_{j,t} \ge 2\left(r_{ij} P_{ij,t} + x_{ij} Q_{ij,t} \right) - M\left(1 - Z_{ij,t}^{\mathrm{L}} \right) - l_{ij,t}\left(x_{ij}^2 + r_{ij}^2 \right) \\ V_{i,t} - V_{j,t} \le 2\left(r_{ij} P_{ij,t} + x_{ij} Q_{ij,t} \right) + M\left(1 - Z_{ij,t}^{\mathrm{L}} \right) - l_{ij,t}\left(x_{ij}^2 + r_{ij}^2 \right) \\ l_{ij,t} = \dfrac{\left(P_{ij,t}^2 + Q_{ij,t}^2 \right)}{V_{i,t}} \end{cases} \tag{30}$$

$$\begin{cases} \left(U_i^{\min} \right)^2 \le V_{i,t} \le \left(U_i^{\max} \right)^2 \\ 0 \le l_{ij,t} \le Z_{ij,t}^{L} \left(I_{ij}^{\max} \right)^2 \end{cases} \tag{31}$$

By using the SOCP methodology on the last equation in (30), the relaxation constraint is presented as follows:

$$\left\| \begin{matrix} 2P_{ij,t} \\ 2Q_{ij,t} \\ l_{ij,t} - V_{i,t} \end{matrix} \right\|_2 \le l_{ij,t} + V_{i,t} \tag{32}$$

Furthermore, the developed model includes terms characterized by absolute values, such as constraints (8), (13) and (14). Without loss of generality, these absolute value terms can be linearized using the following formulation. The first inequality in constraint (33) restricts the permissible increase or decrease in the value of *Z* between time intervals *t* and *t* + 1.

$$\begin{cases} Z_{t+1} - Z_t \le \left(Z^{\max} - Z^{\min} \right) O_t \\ Z_t - Z_{t+1} \le \left(Z^{\max} - Z^{\min} \right) O_t \\ \sum_{t=1}^{T-1} O_t \le \sigma^{\max} \end{cases} \tag{33}$$

where the binary variable O_t is utilized to allow for either an increase or a decrease. $Z^{\max}$ and $Z^{\min}$ are the maximum and minimum values of *Z*. The final inequality imposes a limit on the total number of operational changes (increases or decreases) that can occur throughout the entire time horizon $T-1$. The parameter $\sigma^{\max}$ represents the maximum number of operations permitted, which may reflect budgetary constraints on the frequency of adjustments to *Z* during the operational process.

4.2 Solution Method Based on the Relaxed Cooperative Co-evolution Algorithm

The robust optimization problem addressed in this research is reformulated into a constrained optimization framework through the application of a relaxation evolutionary algorithm [23], [24]. This methodology iteratively alternates between a first-layer minimization and a second-layer maximization, transforming infinite continuous constraints into manageable finite constraints. As an anytime algorithm, it progressively yields increasingly refined solutions over time and computes optimal values for decision variables (x*, representing simulation operation variables) and environmental variables (y*, encompassing load fluctuations and renewable energy outputs) in each iteration, thereby facilitating comprehensive data analysis. By reformulating the intricate continuous min-max problem, the relaxation evolutionary algorithm systematically enhances solution accuracy. Its dual-layer iterative structure enables the simultaneous computation of optimal values for x*, y*, and robustness metrics, rendering it particularly effective for addressing uncertainties in operational environments while providing extensive data for analysis at each stage.

The proposed method involves an iterative process alternating between the first-layer optimization (minmax) and the second-layer optimization (max). In this research, the decision variable x encompasses various simulation operation variables, whereas the environmental variable y comprises load fluctuations and renewable energy output.

(a) The first layer optimization

The first layer of optimization is designed to minimize a variable denoted as ρ, which serves to limit the maximum value of the objective function, as illustrated in equations (34), (35). If maximum value of the objective function f is less than ρ, and ρ obtains the minimum value, then the solution in this layer is found.

$$\underset{x\in \boldsymbol{X}}{\text{minimize}}\ \rho \tag{34}$$

$$\text{s.t.}\begin{cases} f \le \rho, \forall y \in \boldsymbol{Y} \\ (1)-(14),(22)-(33) \end{cases} \tag{35}$$

(b) Relaxation method implementation

Given the continuous nature of the problem, which imposes infinite constraints, it is addressed through relaxation methods that transform it into a series of manageable subproblems. Each subproblem corresponds to a discrete value of the uncertainty variable $y^{(k)}$, selected from a finite set $\boldsymbol{S}_Y$, thereby facilitating the approximation of the solution to the original problem. The optimal value of the objective function, represented as f_m*, along with the corresponding decision variable x^*, is subsequently forwarded to the second layer of optimization for additional analysis.

$$\underset{x\in \boldsymbol{X}}{\text{minimize}}\ \rho$$
$$\text{s.t}\begin{cases} f \le \rho, \forall y^{(k)} \in \boldsymbol{S}_Y \\ (1)-(14),(22)-(33) \\ P_{i,t}^{\mathrm{DG}} = y_{i,t}^{\mathrm{DG},(k)}, Q_{i,t}^{\mathrm{DG}} = P_{i,t}^{\mathrm{DG}} \times \tan\theta, y_{i,t}^{\mathrm{DG},(k)} \in \boldsymbol{S}_Y \\ P_{i,t}^{\mathrm{Load}} = y_{i,t}^{\mathrm{Load},(k)}, y_{i,t}^{\mathrm{Load},(k)} \in \boldsymbol{S}_Y \end{cases} \tag{36}$$

It can be proved that if (x^k, ρ^k) is the optimal solution of the relaxation problem (36), and is also a feasible solution of (34), (35), then this solution is also the optimal solution of (34), (35). If a solution is deemed non-viable, the most serious violation constraint is added to the set $\boldsymbol{S}_Y$. The relaxation evolutionary algorithm then proceeds to approximate the optimal solution by progressively reducing the domain of infeasible solutions.

(c) The second layer of optimization

The second layer of optimization, as formulated in (37), operates under the premise that the decision variables are fixed at their optimal values x* derived from the first layer. In contrast to the first layer, the environmental variables in this layer are unconstrained, encompassing the entire continuous domain Y, rather than being restricted to the finite set $\boldsymbol{S}_Y$. The objective of this layer is to compute the value of the objective function f_M* and to identify the optimal environmental variable y* under worst-case conditions, thereby accounting for the full spectrum of potential uncertainties.

$$\underset{y\in \boldsymbol{Y}}{\text{maximize}}\ f$$
$$\text{s.t}\begin{cases} (1)-(14),(22)-(33) \\ Q_{i,t}^{\mathrm{SVC}} = \hat{x}_{i,t}^{\mathrm{SVC}} \\ Z_{i,t}^{\mathrm{CB}} = \hat{x}_{i,t}^{\mathrm{CB}}, Z_{ij,t}^{\mathrm{L}} = \hat{x}_{ij,t}^{\mathrm{L}} \\ P_{i,t}^{\mathrm{G}} = \hat{x}_{i,t}^{\mathrm{PG}}, Q_{i,t}^{\mathrm{G}} = \hat{x}_{i,t}^{\mathrm{QG}} \\ P_{i,t}^{\mathrm{SOP}} = \hat{x}_{i,t}^{\mathrm{SOP}}, Q_{i,t}^{\mathrm{SOP}} = \hat{x}_{i,t}^{\mathrm{SOP}} \end{cases} \tag{37}$$

(d) The iterative process

The relaxation evolutionary algorithm is implemented as an iterative process. Each iteration involves solving the first layer optimization to obtain (x*, f_m*), updating the lower bound with f_m^*, and subsequently fixing x* to resolve the second layer, yielding (y*, f_M*) and updating the upper bound with f_M^*. The iteration concludes when the difference between f_M* and f_m* falls below a specified threshold, ε_R; otherwise, y* is incorporated into $\boldsymbol{S}_Y$, and the process continues.

5. Case Study

In this section, the modified IEEE 33-bus test system is employed to verify the effectivity of the proposed model and solution algorithm. Note that all the numerical tests are

performed on MATLAB 2022b with Gurobi 10.0.1 on a personal computer with 16 GB RAM and a 2.30 GHz CPU.

5.1 Parameter Setting

A detailed layout of the modified IEEE 33-bus test system utilized in the case study is illustrated in Fig. 3. Voltage stability is assessed within a safe operational range of 0.95 to 1.05 per unit, thereby ensuring the reliability of electrical service. This enhanced system design incorporates contact switches installed across lines 9-15, 8-21, and 25-29, each initially configured in an open state. Furthermore, controllable switches are positioned on lines 12-13, 20-21, and 6-26, starting in a closed condition. Additionally, a two-terminal SOPS device is connected to buses 18 and 33. Other basic parameters can be seen in [25].

The capacity of WT and PV are set at 1 MW and 3 MW respectively. The minimum and maximum value of the reactive power of SVC are –0.1 and 0.1 MVar. The minimum and maximum value of the reactive power of CB are 0 and 0.5 MVar. The minimum and maximum value of the reactive power of SOP are 0 and 0.3 MVar. The ESS within the SOPS is designed with a capacity of 1 MWh. CBs are permitted to perform up to three operations throughout the scheduling horizon. Balancing economic factors with security considerations, the coefficients α and β are established at 0.8 and 0.2, respectively. A representative day is divided into 24 hourly intervals, with each scheduling cycle lasting 1 hour. The parameters for renewable energy and load fluctuations, Λ_{RE} and Λ_{Load}, are set to 8, while the weight factor, ω, is defined as 10%.

5.2 Solution Results

In order to assess the improved efficacy and precision of the proposed algorithm, a comparative analysis was conducted against a traditional robust optimization algorithm [26], as illustrated in Tab. 2. The proposed method is designated as Method 1 (M1), while the conventional approach is referred to as Method 2 (M2). It is significant to note that M1 requires fewer iterations compared to M2. Additionally, the computational time for M1 is only 42.47% of that required by the conventional algorithm, thereby demonstrating the markedly enhanced efficiency of the proposed algorithm.

The optimization results indicate that switches TS1 and D3 maintain a continuous operational state, whereas D1 and TS3 consistently remain disengaged. A notable change occurs with switch D2, which transitions from a closed to an open state at precisely 23:00, a change that is mirrored by TS2. As illustrated in Fig. 4, circuit breaker activations are scheduled for specific times: 15:00, 17:00, and 18:00. Between the hours of 10:00 and 20:00, excess renewable energy is directed to the ESS via the smart operation and planning system, resulting in an upward trend in ESS levels. Conversely, the ESS discharges during periods when there is no surplus of renewable energy.

Method	Obj (p.u.)	Iter No.	Solution time (s)
M1	0.06765	4	205.42
M2	0.06761	7	439.75

Tab. 2. The comparisons of the proposed and traditional approaches.

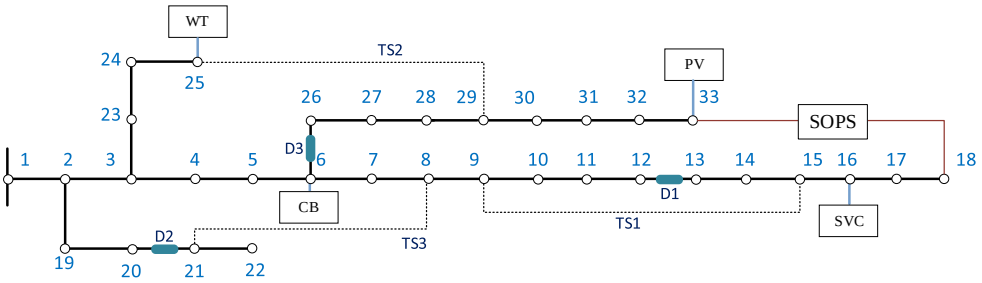

Fig. 3. Diagram of the modified IEEE 33-bus test system.

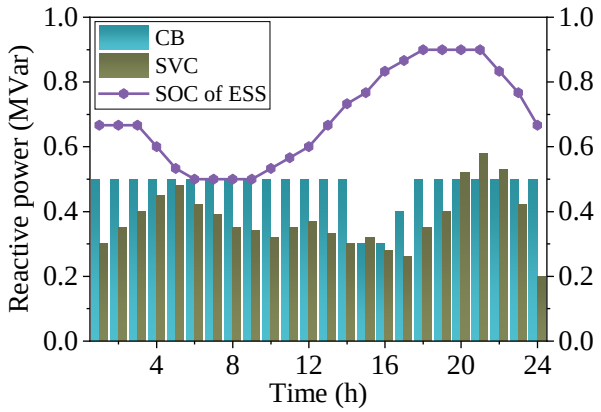

Fig. 4. Operation results of the CB, SVC and ESS.

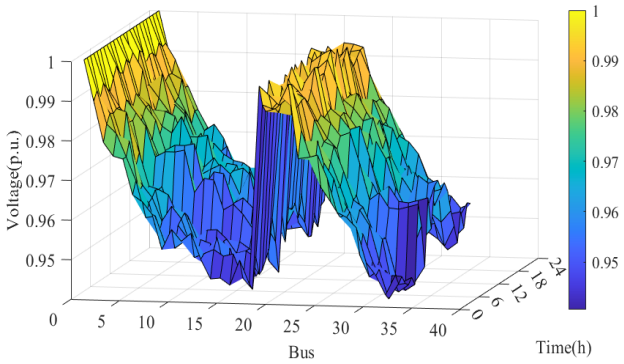

Fig. 5. The fluctuation in voltages at every bus within the system across varying time periods.

Figure 5 demonstrates that the voltages across all buses remain within the safety limits of the operational range. Notably, higher voltage levels are observed at buses numbered 30 to 33 during the midday period from 9:00 to 17:00. The voltages at buses 2 through 12 exhibit consistencies, while those at buses 23 to 33 are predominantly maintained within the range of 0.97 to 1.00 per unit (p.u.) during nighttime and early morning hours, specifically from 1:00 to 8:00, as well as during the late evening from 18:00 to 24:00. The voltages at the remaining buses are generally situated within the range of 1.00 to 1.02 p.u. The fluctuations in terminal voltages can primarily be attributed to the significant output from renewable energy sources, in conjunction with the coordinated application of various active management strategies.

5.3 Computational Performance

The iterative process of the proposed algorithm is detailed in Tab. 3. In this context, f_m and f_M, expressed in per unit (p.u.), represent the optimal results of the objective function for the initial and subsequent optimization phases, respectively. Here, f_M is regarded as the upper bound (UB), while f_m is considered the lower bound (LB). The gap in each iteration can be calculated using the formula |UB – LB|/UB. As indicated in Tab. 2, the convergence criterion, set at less than 5×10^{-4}, is achieved after four rounds of iterative computations.

5.4 Scenario Comparison Analysis

In the second stage of the model, a comprehensive examination is conducted to assess the impact of uncertainties in renewable energy supply and demand on the system. This stage is essential for ensuring the system's resilience against substantial network losses and its capacity to maintain voltage quality standards during extreme conditions. A series of scenarios, as displayed in Tab. 4, are employed to evaluate and validate the model's robustness. Specifically, S1 represents a deterministic model, where ω is set to 0. For S2 and S3, the uncertain parameters are taken as the boundary values of their respective intervals. In S2, the renewable energy output is taken as the upper bound of its interval, while the load is taken as the lower bound. Conversely, in S3, the renewable energy output is taken as the lower bound, and the load is taken as the upper bound. From S4 to S8, different interval change percentages and numbers of adjustments are applied to study the results under various uncertainty scenarios.

By employing a uniform bus system and consistent equipment specifications, the results of the experiments—encompassing metrics such as network loss (P_{loss}), voltage offset (deltV), and the frequency of voltage exceeding permissible limits (Nv_{over}^{limit})—are systematically presented (refer to Fig. 6 and Tab. 5).

In the deterministic model (designated as S1), characterized by high renewable energy penetration, significant voltage deviations are observed, leading to numerous instances of voltage exceeding acceptable limits. In contrast, S2 exhibits increased network losses and diminished economic efficiency relative to S1, although it paradoxically demonstrates smaller voltage deviations; this does not imply enhanced security due to the serious risks posed by voltage over-limit events. S3 reveals the most pronounced voltage deviations and occurrences of voltage falling below acceptable limits, with network losses comparable to those in S2, suggesting similar economic outcomes under varying voltage profiles.

The proposed RO model in Scenarios 4, 5, and 6 significantly mitigates voltage deviations and eradicates in-

#Iter	f_M (UB)	f_m (LB)	Gap (|UB-LB|/UB)
1	0.06765	0.01229	81.84%
2	0.06765	0.05886	12.99%
3	0.06765	0.06286	7.08%
4	0.06765	0.06763	0.03%

Tab. 3. Detailed iteration procedure.

Scenario	Model	Fluctuation deviation	Uncertainties settings
S1	DT	$\omega = 0$	/
S2	/	$\omega = 10\%$	RE takes the upper bound while the load takes the lower bound.
S3	/	$\omega = 10\%$	RE takes the lower bound while the load takes the upper bound.
S4	RO	$\omega = 5\%$	$\Lambda_{RE} = \Lambda_{Load} = 8$
S5	RO	$\omega = 10\%$	$\Lambda_{RE} = \Lambda_{Load} = 8$
S6	RO	$\omega = 15\%$	$\Lambda_{RE} = \Lambda_{Load} = 8$
S7	RO	$\omega = 10\%$	$\Lambda_{RE} = \Lambda_{Load} = 4$
S8	RO	$\omega = 10\%$	$\Lambda_{RE} = \Lambda_{Load} = 16$

Tab. 4. Scenario settings.

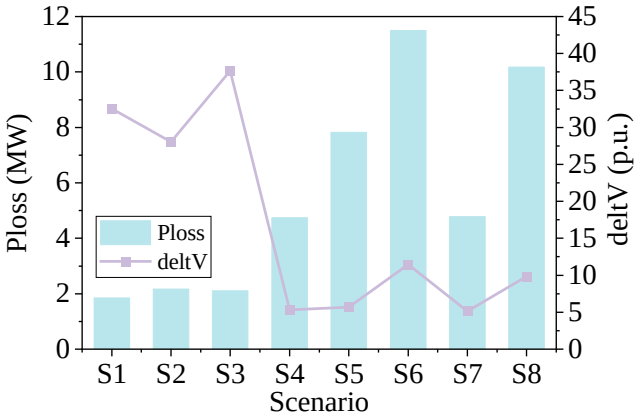

Fig. 6. The network loss and voltage offset in different scenarios.

Scenario	S1	S2	S3	S4	S5	S6	S7	S8
Nv_{over}^{limit}	48	36	112	0	0	0	0	0

Tab. 5. The voltage over-limit number in different scenarios.

stances of voltage exceeding limits, albeit at the cost of slightly reduced economic performance, resulting in more conservative outcomes. An increase in the fluctuation deviation coefficient, ω, across Scenarios 4 to 6 correlates with heightened network losses and voltage deviations, indicating a decline in both economic efficiency and security. Similarly, as the levels of Λ_{RE} and Λ_{Load} rise in Scenarios 5, 7, and 8, network losses and voltage deviations also increase, reflecting a deterioration in system economy and security due to a more cautious approach to managing uncertainties.

5.5 Analysis of Different Portfolios of Regulation Resources

To evaluate the impact of different portfolios of regulation resources on the performance of ADNs, we set up various regulation resource combinations based on S5 in subsection 5.4 and applied the proposed RO model for analysis. The scenario settings are detailed in Tab. 6, where NR means network reconfiguration. Metrics of network loss P_{loss} and voltage offset deltV are displayed in Fig. 5.

From Fig. 7, it can be observed that compared to S5.1, which does not consider any regulation resources, and S5.6, which incorporates all regulation resources, the comprehensive consideration of various regulation resources significantly improves system security and economic efficiency. Specifically, the voltage offset deltV in S5.6 is reduced by 89.6% compared to S5.1, and the network loss P_{loss} is decreased by 12.9%. When comparing S5.2 to 5.6, it is evident that the participation of the SOP and ESS has the best effect on reducing network loss and enhancing voltage quality, followed by the reactive power compensation devices. Meanwhile, the network reconfiguration method demonstrates better performance in improving system security compared to the use of ESS. The comparative analysis of these calculation results indicates that integrating regulation resources into ADNs can improve the economic and security aspects of system operation. Moreover, the coordinated optimization of multiple regulation resources achieves the optimal performance of the system.

5.6 Discussion on Practical Applications

The robust optimization framework proposed in this paper significantly enhances the operational efficiency and stability of ADNs. It achieves this by reducing network losses, improving voltage quality, enhancing economic efficiency and security. The robust optimization framework offers valuable tools for addressing challenges associated with integrating renewable energy into ADNs. Its applicability spans various sectors, from residential and industrial settings to urban and rural environments. For example, this research not only facilitates the coordination of photovoltaic generation with local load demands in residential areas, mitigating power supply instability caused by weather changes, but also applies to microgrid projects in industrial parks, enabling self-sufficiency in electricity supply, increasing energy efficiency, and reducing operational costs.

Cases		S5.1	S5.2	S5.3	S5.4	S5.5	S5.6
SOPS	SOP	×	×	√	√	√	√
	ESS	×	×	×	√	√	√
SVC&CB		×	√	√	×	√	√
NR		×	√	√	√	×	√

Tab. 6. The setting of different portfolios of regulation resources.

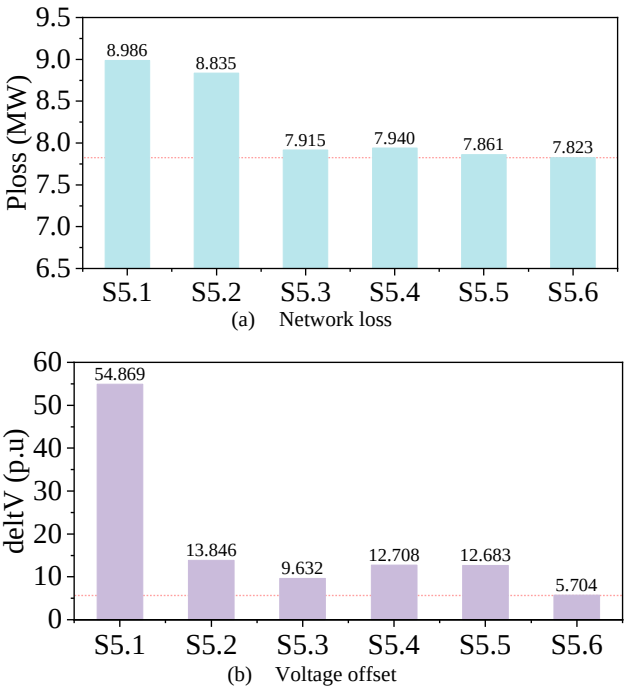

Fig. 7. The network loss (a) and voltage offset (b) in different portfolios of regulation resources.

6. Conclusion

This study presents a comprehensive operational model for distribution networks designed to address uncertainties associated with energy sources and demand. The proposed model incorporates a variety of regulatory resources and employs a relaxation-based evolutionary algorithm for optimization purposes.

Numerical analyses conducted through various test cases indicate that the coordinated scheduling of multiple regulatory resources effectively mitigates uncertainties on both the generation and consumption sides, thereby facilitating optimal integration of renewable energy while keeping voltage fluctuations within acceptable limits. The algorithm demonstrates enhanced efficiency and accuracy, requiring significantly fewer iterations and utilizing only 42.47% of the computational time compared to traditional robust methods. Additionally, the computational performance indicates that the implemented solution algorithm can achieve the specified convergence criteria within

a finite number of iterations. Voltage levels at all buses remain within safe operational thresholds, a result attributed to the output from renewable energy sources and the coordinated management strategies that leverage diverse regulatory resources. Moreover, a comparative analysis across various model scenarios and uncertainty levels reveals that the proposed robust optimization model effectively reduces voltage deviations and mitigates over-limit issues, albeit with minor economic trade-offs, thereby achieving a balance among network losses, voltage stability, and overall system security and economic viability.

Potential research directions include exploring advanced forecasting techniques using machine learning for improved prediction accuracy, expanding uncertainty management to handle extreme events and develop adaptive control strategies, investigating integration with emerging smart grid technologies such as electric vehicles and demand response programs.

Acknowledgments

Funding Statement: This research was funded by Science and Technology project of State Grid Jibei Electric Power Co., LTD. “Demand analysis and operation improvement technology research of county active distribution network for green power consumption improvement” (Project number: B3018K230009).

References

[1] GRUOSSO, G., MAFFEZZONI, P. Data-driven uncertainty analysis of distribution networks including photovoltaic generation. *International Journal of Electrical Power and Energy Systems*, 2020, vol. 121, p. 1–11. DOI: 10.1016/j.ijepes.2020.106043

[2] ZAKERNEZHAD, H., SETAYESH NAZAR, M., SHAFIE-KHAH, M., et al. Optimal scheduling of an active distribution system considering distributed energy resources, demand response aggregators and electrical energy storage. *Applied Energy*, 2022, vol. 314, p. 1–23. DOI: 10.1016/j.apenergy.2022.118865

[3] VAHIDINASAB, V., TABARZADI, M., ARASTEH, A., et al. Overview of electric energy distribution networks expansion planning. *IEEE Access*, 2020, vol. 8, p. 34750–34769. DOI: 10.1109/ACCESS.2020.2973455

[4] GRUOSSO, G., MAFFEZZONI, P., ZHANG, Z., et al. Probabilistic load flow methodology for distribution networks including loads uncertainty. *International Journal of Electrical Power and Energy Systems*, 2019, vol. 106, p. 392–400. DOI: 10.1016/j.ijepes.2018.10.023

[5] DOLATABADI, S. H. H., SOLEIMANI, A., EBTIA, A., et al. Enhancing voltage profile in islanded microgrids through hierarchical control strategies. *Electric Power Systems Research*, 2024, vol. 231, p. 1–11. DOI: 10.1016/j.epsr.2024.110270

[6] CABALLERO-PEÑA, J., CADENA-ZARATE, C., PARRADO-DUQUE, A., et al. Distributed energy resources on distribution networks: A systematic review of modelling, simulation, metrics, and impacts. *International Journal of Electrical Power and Energy Systems*, 2022, vol. 138, p. 1–19. DOI: 10.1016/j.ijepes.2021.107900

[7] YANG, Z., YANG, F., MIN, H., et al. Energy management programming to reduce distribution network operating costs in the presence of electric vehicles and renewable energy sources. *Energy*, 2023, vol. 263, p. 1–12. DOI: 10.1016/j.energy.2022.125695

[8] GHAEMI, S., SALEHI, J., MOEINI-AGHTAIE, M. Estimating abilities of distributed energy resources in providing flexible ramp products for active distribution networks. *Sustainable Cities and Society*, 2021, vol. 65, p. 1–14. DOI: 10.1016/j.scs.2020.102593

[9] SHAFIK, M. B., CHEN, H., RASHED, G. I., et al. Adequate topology for efficient energy resources utilization of active distribution networks equipped with soft open points. *IEEE Access*, 2019, vol. 7, p. 99003–99016. DOI: 10.1109/ACCESS.2019.2930631

[10] DAS, A., SENGUPTA, A. Power system voltage stabilization using model predictive control. *Electrical Engineering*, 2024, vol. 106, no. 3, p. 2765–2783. DOI: 10.1007/s00202-023-02099-5

[11] GARRIDO-ARÉVALO, V. M., GIL-GONZÁLEZ, W., MONTOYA, O. D., et al. Optimal dispatch of DERs and battery-based ESS in distribution grids while considering reactive power capabilities and uncertainties: A second-order cone programming formulation. *IEEE Access*, 2024, vol. 12, p. 48497–48510. DOI: 10.1109/ACCESS.2024.3382940

[12] MAHDAVI, M., SCHMITT, K., CHAMANA, M., et al. A mixed-integer programming model for reconfiguration of active distribution systems considering voltage dependency and type of loads and renewable sources. *IEEE Transactions on Industry Applications*, 2024, vol. 60, no. 4, p. 5291–5303. DOI: 10.1109/TIA.2024.3383805

[13] SHARMA, S., NIAZI, K. R., VERMA, K., et al. Impact of battery energy storage, controllable load and network reconfiguration on contemporary distribution network under uncertain environment. *IET Generation, Transmission & Distribution*, 2020, vol. 14, no. 21, p. 4719–4727. DOI: 10.1049/iet-gtd.2020.0369

[14] MARDANIMAJD, K., KARIMI, S., ANVARI-MOGHADDAM, A. Voltage stability improvement in distribution networks by using soft open points. *International Journal of Electrical Power and Energy Systems*, 2024, vol. 155, p. 1–17. DOI: 10.1016/j.ijepes.2023.109582

[15] YIN, Z., WANG, S., ZHAO, Q. Sequential reconfiguration of unbalanced distribution network with soft open points based on deep reinforcement learning. *Journal of Modern Power Systems and Clean Energy*, 2023, vol. 11, no. 1, p. 107–119. DOI: 10.35833/MPCE.2022.000271

[16] JIANG, X., ZHOU, Y., MING, W., et al. An overview of soft open points in electricity distribution networks. *IEEE Transactions on Smart Grid*, 2022, vol. 13, no. 3, p. 1899–1910. DOI: 10.1109/TSG.2022.3148599

[17] SARANTAKOS, I., PEKER, M., ZOGRAFOU-BARREDO, N. M., et al. A robust mixed-integer convex model for optimal scheduling of integrated energy storage—soft open point devices. *IEEE Transactions on Smart Grid*, 2022, vol. 13, no. 5, p. 4072 to 4087. DOI: 10.1109/TSG.2022.3145709

[18] HU, R., WANG, V., CHEN, Z., et al. Coordinated voltage regulation methods in active distribution networks with soft open points. *Sustainability*, 2020, vol. 12, no. 22, p. 1–18. DOI: 10.3390/su12229453

[19] MA, H., LIU, Z., LI, M., et al. A two-stage optimal scheduling method for active distribution networks considering uncertainty risk. *Energy Reports*, 2021, vol. 7, p. 4633–4641. DOI: 10.1016/j.egyr.2021.07.023

[20] LENG, R., LI, Z., XU, Y. Two-stage stochastic programming for coordinated operation of distributed energy resources in

unbalanced active distribution networks with diverse correlated uncertainties. *Journal of Modern Power Systems and Clean Energy*, 2023, vol. 11, no. 1, p. 120–131. DOI: 10.35833/MPCE.2022.000510

[21] XU, T., REN, Y., GUO, L., et al. Multi-objective robust optimization of active distribution networks considering uncertainties of photovoltaic. *International Journal of Electrical Power and Energy Systems*, 2021, vol. 133, p. 1–10. DOI: 10.1016/j.ijepes.2021.107197

[22] YANG, J., GUO, Y., GUO, C., et al. A robust active distribution network defensive strategy against cyber-attack considering multi-uncertainties. *IET Generation, Transmission and Distribution*, 2022, vol. 16, no. 8, p. 1476–1488. DOI: 10.1049/gtd2.12443

[23] ANTONIOU, M., PAPA, G. Solving min-max optimisation problems by means of bilevel evolutionary algorithms: A preliminary study. In *Proceedings of the 2020 Genetic and Evolutionary Computation Conference Companion GECCO '20.* New York (NY, USA), 2020, p. 187–188. DOI: 10.1145/3377929.3390037

[24] XU, B., GONG, D., SHANG, Y., et al. Cooperative co-evolutionary algorithm for multi-objective optimization problems with changing decision variables. *Information Sciences*, 2022, vol. 607, p. 278–296. DOI: 10.1016/j.ins.2022.05.123

[25] https://www.torontomu.ca/content/dam/cue/research/reports/33bus%20test%20system.pdf.

[26] CAI, X., HUANG, Q., ZHOU, X., et al. Multi-objective dynamic reactive power optimization based on OLTC and reactive power compensation. In *2022 4th Asia Energy and Electrical Engineering Symposium (AEEES)*. Chengdu (China), 2022, p. 825–831. DOI: 10.1109/AEEES54426.2022.9759406

About the Authors ...

DING Ran was born in 1987. He received his master's degree in Electrical Engineering from Tsinghua University in 2012. Currently, he is pursuing a doctoral degree in the Department of Electrical Engineering at Tsinghua University. His research areas include power system dispatch and operation, large-scale new energy grid integration, prediction and coordinated control, as well as source-grid-load-storage coordinated optimization.

Lin CHENG (Senior Member, IEEE), was born in1973. He received the B.S. degree in Electrical Engineering from Tianjin University, Tianjin, China, in 1996 and the Ph.D. degree from Tsinghua University, Beijing, China, in 2001. Currently, he is a tenured Professor in the Department of Electrical Engineering at Tsinghua University, serving as the deputy director of the State Key Laboratory of Power System Operation and Control, and is also a Fellow of IET. His research interests include operational reliability evaluation and application of power systems, operation optimization of distribution systems with flexible resources, and perception and control of uncertainty in wide-area measurement systems.

WANG Xuanyuan was born in 1979. She obtained her Ph.D. in Electrical Engineering from Tsinghua University in 2019 and is a professor-level senior engineer. Currently, she works at State Grid Jibei Electric Power Co., Ltd. Her research areas include power system dispatch and operation, power markets, large-scale power grid security and stability control, and coordinated optimization of generation, transmission, load and storage.

YAO Yiming was born in 1993. He received his Master's degree in Electrical Engineering from Tsinghua University in 2017 and is an engineer. Currently, he works at State Grid Jibei Electric Power Co., Ltd. His research areas include power system dispatch and operation, large-scale renewable energy grid integration, prediction and coordinated control, and new energy storage dispatch and operation.

XU Haixiang was born in 1988. He obtained his Master's degree in Power System Automation from North China Electric Power University in 2014 and is a senior engineer. Currently, he works at State Grid Jibei Electric Power Co., Ltd. His research areas include power system dispatch and operation, distributed renewable energy operation, and coordinated optimization of generation, transmission, load and storage.

Ergang ZHAO (corresponding author) was born in 1991. He received the bachelor's degree in Electrical Engineering from Hebei of University Technology in 2014 and the master's degree in Electrical Engineering from Tsinghua University in 2021, respectively. He is currently working as a researcher at the Department of Electrical Engineering, Tsinghua University. His research areas include power system operation and planning, microgrid operation.